J|A|C|S ARTICLES

Published on Web 03/24/2009

Accurate Solution Structures of Proteins from X-ray Data and a Minimal Set of NMR Data: Calmodulin−Peptide Complexes As Examples

Ivano Bertini,*[,†,‡] Petri Kursula,[§,||] Claudio Luchinat,[†,⊥] Giacomo Parigi,[†,⊥] Juha Vahokoski,[§] Matthias Wilmanns,[§] and Jing Yuan[†]

Magnetic Resonance Center (CERM), University of Florence, Via Luigi Sacconi 6, 50019 Sesto Fiorentino, Italy, Department of Chemistry, University of Florence, Via della Lastruccia 3, 50019 Sesto Fiorentino, Italy, EMBL-Hamburg c/o DESY, Hamburg, Germany, Department of Biochemistry, University of Oulu, Oulu, Finland, and Department of Agricultural Biotechnology, University of Florence, via Maragliano 75-77, 50144 Florence, Italy

Received October 14, 2008; E-mail: ivanobertini@cerm.unifi.it

Abstract: A strategy for the accurate determination of protein solution structures starting from X-ray data and a minimal set of NMR data is proposed and successfully applied to two complexes of calmodulin (CaM) with target peptides not previously described. Its implementation in the present case is based on the use of lanthanide ions as substitutes for calcium in one of the four calcium binding sites of CaM and the collection of pseudocontact shift (pcs) and residual dipolar coupling (rdc) restraints induced by the paramagnetic metals. Starting from the crystal structures, new structural models are calculated that are in excellent agreement with the paramagnetic restraints and differ significantly from the starting crystal structures. In particular, in both complexes, a change in orientation of the first helix of the N-terminal CaM domain and of the whole C-terminal domain is observed. The simultaneous use of paramagnetic pcs and rdc restraints has the following crucial advantages: (i) it allows one to assess the possible presence of interdomain conformational freedom, which cannot be detected if the rdc values are derived from external orienting media; (ii) in the absence of significant conformational freedom, the global orientation tensor can be independently and precisely determined from pcs values, which are less sensitive than rdc values to the presence of local structural inaccuracies, and therefore (iii) the *relative* rearrangement of a domain or a secondary structure element with respect to the metal-bearing domain can be detected.

Introduction

Soluble proteins perform their function in solution, and therefore, it is crucial to obtain detailed information about their structure in solution. NMR can yield such structures provided that the size of the protein is not too large. However, NMR structures are not very precise because of the relatively few experimental restraints which are also loose in nature. On the other hand, crystallographic structures are numerous, precise, and reliable, and they are taken as models of solution structures. When the two structures of the same molecule are compared, often the solution structure within its indetermination is equal to the solid state structure. Sometimes, certain residues may reorient in solution or conformational equilibria may be detected. Attempts have been made to measure a set of NMR restraints in solution and to take them to adapt or refine the crystal structure toward a solution model.[1,2]

The residual dipolar couplings (rdc) are optimally suited to detect global structural features, especially relative orientations of secondary structural elements or entire domains.[2−8] However, they are ambiguous in nature, affected by motions, and hardly usable for structural purposes in the presence of conformational equilibria.[9−11] To overcome such drawbacks, rdc experiencing conformational mobility can be removed, a number of different orienting media can be used, and a number of sets of rdc can be measured (e.g., NH, CH, etc.).

The problem is even more complicated in the presence of mobile domains. Calmodulin (CaM), with its C- and N-terminal domains connected by a flexible linker, is a paradigmatic

† Magnetic Resonance Center (CERM), University of Florence.
‡ Department of Chemistry, University of Florence.
§ EMBL-Hamburg c/o DESY.
|| University of Oulu.
⊥ Department of Agricultural Biotechnology, University of Florence.

(1) Gochin, M.; Roder, H. *Protein Sci.* **1995**, *4*, 296–305.
(2) Chou, J. J.; Li, S.; Klee, C. B.; Bax, A. *Nat. Struct. Biol.* **2001**, *8*, 990–997.
(3) Fowler, B. A.; Tian, F.; Al-Hashimi, H. M.; Prestegard, J. H. *J. Mol. Biol.* **2000**, *304*, 447–460.
(4) Skrynnikov, N. R.; Goto, N. K.; Yang, D.; Choy, W.-Y.; Tolman, J. R.; Mueller, G. A.; Kay, L. E. *J. Mol. Biol.* **2000**, *295*, 1265–1273.
(5) Tolman, J. R.; Flanagan, J. M.; Kennedy, M. A.; Prestegard, J. H. *Nat. Struct. Biol.* **1997**, *4*, 292–297.
(6) Bertini, I.; Del Bianco, C.; Gelis, I.; Katsaros, N.; Luchinat, C.; Parigi, G.; Peana, M.; Provenzani, A.; Zoroddu, M. A. *Proc. Natl. Acad. Sci. U.S.A.* **2004**, *101*, 6841–6846.
(7) Bertini, I.; Gupta, Y. K.; Luchinat, C.; Parigi, G.; Peana, M.; Sgheri, L.; Yuan, J. *J. Am. Chem. Soc.* **2007**, *129*, 12786–12794.
(8) Pintacuda, G.; Park, A. Y.; Keniry, M. A.; Dixonj, N. E.; Otting, G. *J. Am. Chem. Soc.* **2006**, *128*, 3696–3702.
(9) Tolman, J. R.; Al-Hashimi, H. M.; Kay, L. E.; Prestegard, J. H. *J. Am. Chem. Soc.* **2001**, *123*, 1416–1424.
(10) Meiler, J.; Prompers, J. J.; Peti, W.; Griesinger, C.; Bruschweiler, R. *J. Am. Chem. Soc.* **2001**, *123*, 6098–6107.
(11) Tolman, J. R. *J. Am. Chem. Soc.* **2002**, *124*, 12020–12030.

 10.1021/ja8080764 CCC: $40.75

example.[6,7] Rdc can provide structural information on the two domains separately,[2] but with external orienting media no information is available on the population of their conformational space because each domain interacts independently with the orienting media. In this case, some progress can be made with the exploitation of lanthanides incorporated into the protein as orienting media. Lanthanides can in certain conditions bind within a calcium binding site of the N-terminal domain of CaM and partially orient it. Furthermore, if the C-terminal domain is not completely free to rotate (as it is), then some reduced partial orientation is experienced also by such a domain.

When CaM binds to a protein ligand, or to a peptide representing it, the two domains may be rigid or mobile. Furthermore, if rigid, they may reorient from solid to solution. We propose here that multiple lanthanides as orienting devices may give the correct answer. In fact, the fitting of rdc can provide a model of the protein structure in solution more accurate than the crystal structure if the orienting tensor is known independently, and in the case of lanthanides, the orienting tensor is the magnetic susceptibility anisotropy, which in turn can be obtained from pseudocontact shifts (pcs).[12,13] This is a general approach, as lanthanides can be either inserted into one domain of the molecule or attached through a rigid tag.[14−17] We show that some significant rearrangements do occur between the solid and solution states for the adduct between CaM and two different synthetic peptides, representing the CaM-binding sites of two protein partners, the death-associated protein kinase (DAPk) and the DAPk-related protein 1 (DRP-1).[18] Such an approach, i.e., finding the orienting tensor from other observables (pcs) and using rdc to calculate a solution structure starting from a crystallographic structure, is unprecedented.

Materials and Methods

Sample Preparation, Crystallization, and Structure Solution. Human CaM was expressed in *E. coli* and purified by Ca-dependent hydrophobic interaction chromatography on phenyl sepharose. The peptide RRRWKLSFSIVSLCNHLTR, representing the amino acid sequence of the CaM-binding domain of DRP-1 (residues 302−320), was purchased from Mimotopes. Crystallization was carried out at +20 °C by vapor diffusion, in sitting drops containing 1 μL of protein−peptide mixture (0.5 mM CaM, 1.5 mM peptide in 20 mM $CaCl_2$, 50 mM HEPES, pH 7.5) and 1 μL of well solution. The optimal well solution contained 30% PEG 1500, 10 mM DTT, and 0.1 M sodium acetate (pH 4.8). Data were collected at 100 K on beamline X13 at EMBL-Hamburg/DESY. The diffraction data were processed using XDS[19] and XDSi.[20] Initial phasing was carried out by molecular replacement in MOLREP,[21] using the N- and C-terminal domains of CaM separately. Refinement was performed using REFMAC5[22] with TLS parameters.[23] Model building and analysis were done in O.[24] Water molecules were added both manually and with Arp/Warp.[25] Residues 2−148 of CaM and all residues of the peptide were built into the model. The processing and refinement statistics are shown in Tables S1−S2 in the Supporting Information. The coordinates and structure factors were deposited at the Protein Data Bank with the accession code 1WRZ.

^{15}N and ^{13}C labeled N60D CaM was purchased from ProtEra srl (Florence, Italy, www.proterasrl.com). NMR samples of Ca_4CaM and $LnCa_3$CaM (Ln = Tb, Tm, Yb, and Dy) were prepared as previously reported[6,7] (HEPES 30 mM, KCl 200 mM, TCEP 3 mM pH 7.4). CaM concentration was 0.5 mM; peptides were in slight excess.

NMR Measurements. ^{1}H−^{15}N HSQC experiments were performed at 700 MHz. Pcs data were obtained as the ^{1}H and ^{15}N chemical shift difference between the paramagnetic form and the diamagnetic form. Rdc data were obtained from IPAP experiments[26] at 700 MHz as the difference in the doublet splitting in the indirect ^{15}N dimension between the paramagnetic form and the diamagnetic form. HNCO, HNCA, HN(CO)CA, and CBCA(CO)NH spectra for backbone assignment were acquired on a Bruker 500 MHz spectrometer equipped with a cryoprobe. ^{15}N relaxation rates (R_1 and R_2) were measured at 70.94 MHz ^{15}N base frequency using standard pulse schemes[27,28] to collect 10 points with delays of 2.5, 75, 125, 275, 400, 500, 600, 850, 1500, 2000 ms for R_1 and 9 points with delays of 16.96, 33.92, 50.88, 67.84, 84.80, 118.72, 152.64, 186.56, 237.44 ms for R_2. Relaxation delays were 3.0 s for both R_1 and R_2 measurements. Relaxation rates were determined by fitting the crosspeak heights, obtained through the standard routine of the Sparky program.[29] All experiments were performed at 298 K.

Use of Paramagnetism-Based Restraints. The ^1J splittings of coupled nuclei can experience dipolar contributions, due to partial self-orientation of the investigated system in the magnetic field. In the present case, the partial orientation is due to the magnetic susceptibility anisotropies of the lanthanides, $\Delta\chi_{ax}$ and $\Delta\chi_{rh}$. Such contributions are called residual dipolar couplings (rdc) and provided by eq 1.[30,31]

$$\mathrm{rdc(Hz)} = -\frac{1}{4\pi}\frac{B_0^2}{15kT}\frac{\gamma_N\gamma_H\hbar}{2\pi r_{HN}^3}\left[\Delta\chi_{ax}(3\cos^2\theta - 1) + \frac{3}{2}\Delta\chi_{rh}\sin^2\theta\cos 2\phi\right] \quad (1)$$

where r_{HN} is the distance between the two coupled nuclei N and ^{N}H, and the polar angles θ and ϕ are those defining the orientation of the vector connecting the coupled nuclei in the frame of the magnetic susceptibility tensor. Other symbols have the usual meaning. Therefore, rdc are related to the orientation of the vector connecting the coupled nuclei in the reference frame of the magnetic susceptibility tensor axes and to the extent of the magnetic anisotropy.[5,32−34]

(12) Bertini, I.; Luchinat, C.; Parigi, G.; Pierattelli, R. *ChemBioChem* **2005**, *6*, 1536–1549.
(13) Bertini, I.; Luchinat, C.; Parigi, G.; Pierattelli, R. *Dalton Trans.* **2008**, *2008*, 3782–3790.
(14) Su, X. C.; Huber, T.; Dixon, N. E.; Otting, G. *ChemBioChem* **2006**, *7*, 1599–1604.
(15) Su, X. C.; Man, B.; Beeren, S.; Liang, H.; Simonsen, S.; Schmitz, C.; Huber, T.; Messerle, B. A.; Otting, G. *J. Am. Chem. Soc.* **2008**, *130*, 10486–10487.
(16) Vlasie, M. D.; Fernández-Busnadiego, R.; Prudêncio, M.; Ubbink, M. *J. Mol. Biol.* **2008**, *375*, 1405–1415.
(17) Zhuang, T.; Lee, H. S.; Imperiali, B.; Prestegard, J. H. *Protein Sci.* **2008**, *17*, 1220–1231.
(18) Cohen, O.; Feinstein, E.; Kimchi, A. *EMBO J.* **1997**, *16*, 998–1008.
(19) Kabsch, W. *J. Appl. Crystallogr.* **1993**, *26*, 795–800.
(20) Kursula, P. *J. Appl. Crystallogr.* **2004**, *37*, 347–348.
(21) Vagin, A.; Teplyakov, A. *J. Appl. Crystallogr.* **1997**, *30*, 1022–1025.
(22) Murshudov, G. N.; Vagin, A. A.; Dodson, E. J. *Acta Crystallogr., Sect. D* **1997**, *53*, 240–255.
(23) Winn, M. D.; Isupov, M. N.; Murshudov, G. N. *Acta Crystallogr., Sect. D* **2001**, *57*, 122–133.
(24) Jones, T. A.; Zou, J. Y.; Cowtan, S. W.; Kjeldgaard, M. *Acta Crystallogr., Sect. A* **1991**, *47*, 110–119.
(25) Perrakis, A.; Morris, R. J. H.; Lamzin, V. S. *Nat. Struct. Biol.* **1999**, *6*, 458–463.
(26) Ottiger, M.; Delaglio, F.; Bax, A. *J. Magn. Reson.* **1998**, *131*, 373–378.
(27) Kay, L. E.; Torchia, D. A.; Bax, A. *Biochemistry* **1989**, *28*, 8972–8979.
(28) Barbato, G.; Ikura, M.; Kay, L. E.; Pastor, R. W.; Bax, A. *Biochemistry* **1992**, *31*, 5269–5278.
(29) Goddard, T. D.; Kneller, D. G. *SPARKY 3*; University of California: San Francisco, 2000. Ref Type: Computer Program
(30) Bertini, I.; Luchinat, C.; Parigi, G. *Progr. NMR Spectrosc.* **2002**, *40*, 249–273.
(31) Banci, L.; Bertini, I.; Huber, J. G.; Luchinat, C.; Rosato, A. *J. Am. Chem. Soc.* **1998**, *120*, 12903–12909.

The information on the magnetic susceptibility anisotropy may be independently obtained from pseudocontact shifts (pcs). They are related to the magnetic anisotropies and to the structural parameters through eq 2[30]

$$\mathrm{pcs} = \frac{1}{12\pi r^3}\left[\Delta\chi_{\mathrm{ax}}(3\cos^2\Theta - 1) + \frac{3}{2}\Delta\chi_{\mathrm{rh}}\sin^2\Theta\cos 2\Phi\right] \quad (2)$$

where r is the distance between observed nuclei and metal ion, and Θ and Φ identify the polar coordinates of the nucleus in the frame of the magnetic susceptibility tensor. Therefore, pcs are related to the position of the nuclei with respect to both the metal ion and the magnetic susceptibility tensor, besides the value of the anisotropies of the latter.

Discarding Mobile Residues. Some $N-^{N}H$ vectors may undergo major reorientations in the NMR time scale, and therefore the corresponding rdc are useless as structural restraints. NMR relaxation data can detect such reorientations in the milli- to microsecond and nano- to picosecond time scales. R_1 and R_2 data[27] were thus recorded and analyzed to discard the NHs experiencing such mobility (Figures S1 and S2). An R_2 value or R_2/R_1 ratio larger than that calculated with HYDRONMR[35] is in particular observed for some residues, mainly residues of the first helix of the C-terminal domain and/or interacting with the bound peptide (residues 24, 39, 92, 93, 122, 127, 141, 144, and 145 in the DAPk case and residues 16, 64, 87, 93, and 96 in the DRP-1 case): these residues are thus expected to experience motions in the microsecond to millisecond time scale.[27,36] As already noted for CaM bound to the CaMKI peptide, these data account for significant contributions from chemical exchange phenomena.[37] Large mobility is also observed for the residues in the linker between the N-terminal and C-terminal domains and for residues 42, 57, 113−116, 130, 137, and 138 (all in protein loops, see Table S10 in the Supporting Information), consistent with previous measurements performed for CaM complexed with other peptides.[28,37−39] Of course, to test the applicability of the present strategy, data affected by sizable mobility need to be discarded.

Obtaining the Structure in Solution. The protein structures in solution were refined using the crystal structures as starting models and correcting them by applying the NMR restraints. First, the magnetic susceptibility anisotropy tensors were obtained from eq 2 by using pcs and the crystallographic structures of the N-terminal domain. In fact, pcs are much less sensitive than rdc to both mobility and local structural inaccuracies.[40] A simulation to exemplify the different features of the two types of restraints is reported in the Supporting Information (Figure S3). Then, the N-terminal crystallographic structure was refined using both pcs and rdc and the routine PARArestraints for Xplor-NIH through the refinement protocol described below.[41] For each run the magnetic susceptibility anisotropies are fixed to the previously calculated values, and the tensors are represented by properly defined pseudoresidues. Pcs restraints were given a large weight, to prevent the directions of the magnetic susceptibility tensors to be determined by rdc. The orienting magnetic susceptibility anisotropy tensors are then recalculated through eq 2 and the calculations repeated, until the magnetic susceptibility anisotropy tensors are invariant and the new structure for the N-terminal domain is obtained. Three runs were sufficient to achieve convergence. The refined structure of the whole protein was then obtained with the same refinement protocol using the rdc of the C-terminal domain, the refined structure of the N-terminal domain, and the pcs measured on the latter to fix the magnetic susceptibility tensors. The indetermination of the calculated structure was estimated by performing multiple calculations after perturbing the pcs and rdc with a stochastic error of 0.1 ppm and 1.5 Hz, respectively.

The refinement protocol was based on subjecting the crystal structure to a simulated annealing at 100 K, restrained at the backbone torsion ϕ and Ψ angles extracted from the structure itself, to minimize it with respect to the employed library (topology and parameter files were topallhdg5.3 and parallhdg5.3, respectively). This determined a slight rearrangement in the protein structure (with amplitude smaller than 0.5 Å of backbone rmsd). As a second step, an internal dynamics at 200 K and a minimization were performed, with the force constant of the starting backbone ϕ and Ψ torsion angle restraints ramped down, with the addition of the pcs restraints with a force constant of 41.87 kJ mol^{-1} ppm^{-2} and of the rdc restraints with force constant of 0.837 and 3.35 kJ mol^{-1} Hz^{-2} for Tb^{3+}, Tm^{3+}, and Dy^{3+} and for Yb^{3+}, respectively (the force constant for Yb rdc was set larger than that for the other metals because of the smaller values of Yb rdc). The much larger weights provided to pcs restraints ensure that the directions of the magnetic susceptibility tensors are essentially fixed by such restraints rather than by rdc. Rdc were calculated through eq 1, where an order parameter $S = 1$ is assumed. The structural results were indeed insensitive to changes of S down to $S = 0.9$ (S^2 ca. 0.8). Dihedral angle restraints calculated with TALOS (with force constant of 1256 kJ mol^{-1} rad^{-2}) were also added in one set of calculations, but the resulting structures were indistinguishable from those obtained without such restraints. Even if the calculations were performed in the absence of NOEs, no expansion in the volume of the protein domains was observed. In summary, the protocol consists of a refinement of the crystal structure performed at low temperature to have the smallest changes required for the best agreement of all the experimental paramagnetism-based restraints. A large uncertainty results in the linker region (residues 77−82 and 76−85 for the DAPk complex and the DRP-1 complex, respectively) because all residues in that region experience mobility and the corresponding rdc values were discarded.

Results and Discussion

Crystal Structures. The 1.7-Å crystal structure of Ca^{2+}-bound CaM complexed with a peptide (RKKWKQSVRLISLCQRLSR) from the corresponding domain of DAPk (PDB entry 1YR5) was analyzed; in addition, the crystal structure of CaM complexed with the DRP-1 peptide was determined at a 2.0 Å resolution. The N- and C-terminal CaM domains wrap around the bound peptide, which has an α-helical structure, according to the canonical closed state. The peptides bind in an antiparallel orientation, i.e., with the N- and C-terminal CaM domains interacting mainly with the C- and N-terminal halves of the peptide, respectively. The same orientation was observed for peptides derived from MLCK[42,43] and from CaM-dependent protein kinase II.[44]

(32) Tolman, J. R.; Flanagan, J. M.; Kennedy, M. A.; Prestegard, J. H. *Proc. Natl. Acad. Sci. U.S.A.* **1995**, *92*, 9279–9283.
(33) Bax, A.; Tjandra, N. *Nat. Struct. Biol.* **1997**, *4*, 254–256.
(34) Bothner-By, A. A.; Domaille, J. P.; Gayathri, C. *J. Am. Chem. Soc.* **1981**, *103*, 5602–5603.
(35) de la Torre, J. G.; Huertas, M. L.; Carrasco, B. *J. Magn. Reson.* **2000**, *147*, 138–146.
(36) Larsson, G.; Martinez, G.; Schleucher, J.; Wijmenga, S. S. *J. Biomol. NMR* **2004**, *27*, 291–312.
(37) Frederick, K. K.; Kranz, J. K.; Wand, A. J. *Biochemistry* **2006**, *45*, 9841–9848.
(38) Wang, T.; Frederick, K. K.; Igumenova, T. I.; Wand, A. J.; Zuiderweg, E. R. P. *J. Am. Chem. Soc.* **2005**, *127*, 828–829.
(39) Marlow, M. S.; Wand, A. J. *Biochemistry* **2006**, *45*, 8732–8741.
(40) Assfalg, M.; Bertini, I.; Turano, P.; Mauk, A. G.; Winkler, J. R.; Gray, B. H. *Biophys. J.* **2003**, *84*, 3917–3923.
(41) Banci, L.; Bertini, I.; Cavallaro, G.; Giachetti, A.; Luchinat, C.; Parigi, G. *J. Biomol. NMR* **2004**, *28*, 249–261.
(42) Ikura, M.; Clore, G. M.; Gronenborn, A. M.; Zhu, G.; Clee, C.; Bax, A. *Science* **1992**, *256*, 632–638.
(43) Meador, W. E.; Means, A. R.; Quiocho, F. A. *Science* **1992**, *257*, 1251–1255.

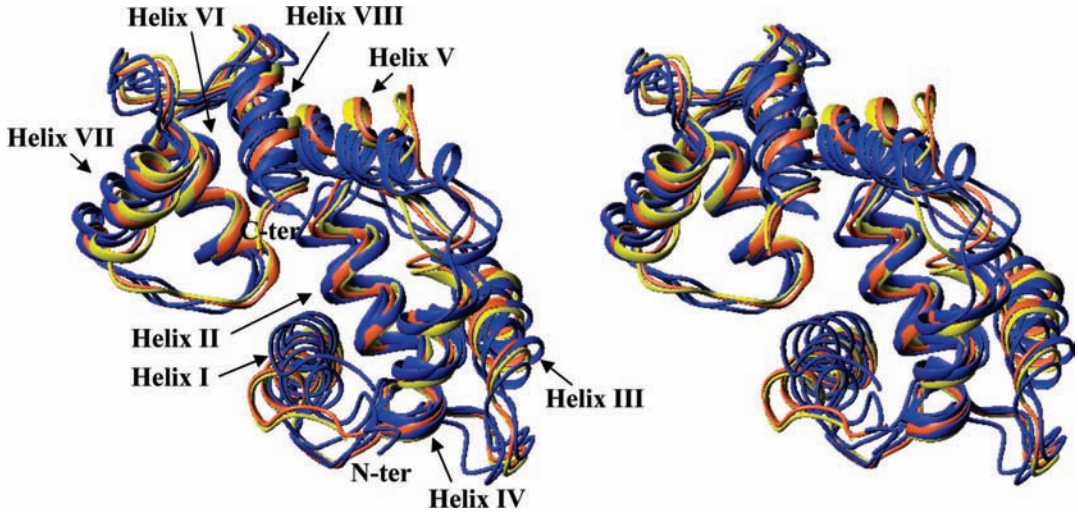

Figure 1. Stereoview of the crystal structures of CaM bound to DAPk (in yellow) or to DRP-1 (in orange) peptides superimposed to the PDB structures 1CDL, 1NIW, and 1SY9 (in blue).

The complex is stabilized by several hydrophobic interactions. Tryptophan 305 and leucine 318 mainly act to anchor the peptide to the hydrophobic patches of CaM. In addition to the hydrophobic interactions, there are a number of possible electrostatic interactions, such as those between peptide arginines and lysines and CaM glutamate residues in helices I and VII.

The mechanism of activation by CaM is common for all its protein-derived peptide targets. However, four different recognition modes have been identified, termed 1−10, 1−14, 1−16, or 1−17 motifs, based on the position of the two key anchoring hydrophobic residues in the target peptide.[45,46] A fifth interaction motif has been described for the gating domain of the small conductance Ca^{2+}-activated K^+ channels.[47] The recognition mode for DAPk and DRP-1 corresponds to the 1−14 motif. The same motif has been identified for the skeletal muscle and smooth muscle MLCK peptides[42,43] (PDB 1CDL), the endothelial nitric oxide synthase peptide[48] (1NIW), and a peptide derived from the olfactory CNG channel[49] (1SY9). A comparison among the CaM structures in these complexes with respect to the structures determined for the complex with DAPk or DRP-1 peptides shows that all structures are in an overall agreement (see Figure 1). However, some small structural differences can be noticed. In particular, the first helix of the N-terminal domain can be differently oriented depending on the bound peptide. It has already been noted that this depends on the specific interactions between the binding peptide and the first helix residues.[48]

Of relevance to the present study are the intermolecular interactions that connect each CaM peptide complex with the neighboring molecules in the crystal. Such interactions, lacking in solution, deserve a systematic analysis, as they may be the cause of any possible structural difference between the crystal structure and the solution structure of the complexes. Table S11 lists all H-bond, salt bridge, and van der Waals contacts between each complex and its neighbors in the crystalline state. It can be noted that a number of hydrogen bonds are present between the N-terminal and neighbor molecules 3, 5, and 7, those with molecule 3 involving helix 1, those with molecule 5 involving helix 3, and those with molecule 7 involving helices 1 and 4 of the N-terminal domain. These interactions are similar in the two complexes. In addition, a salt bridge between glutamates 7 and 14 and arginine 302 in DAPk, between glutamates 7 and 14 and arginine 303, and between glutamate 11 and lysine 306 in DRP-1 establish contacts between the N-terminal domain and the peptide, helping the maintenance of the closed conformation of the complex. A summary of the relevant interactions is schematically shown in Figure 2.

Choice, Collection of Paramagnetic Restraints, and Strategy. Equation 1 provides a relationship among the structure, the orienting tensors, and the rdc. Provided with a structure and a $\Delta\chi$ orienting tensor, e.g., originated by a lanthanide, rdc are univocally determined through eq 1. However, the determination of the structure from $\Delta\chi$ and rdc is not univocal. In fact, if for simplicity an axial orienting tensor is considered ($\Delta\chi_{rh} = 0$), from one rdc there are infinite directions of the N−H vectors, the only restraint being that they lie on the surface of a double right circular cone forming an angle of θ and $180-\theta$ with the z direction, respectively. Therefore, a set of rdc values can be safely used for solution structure refinement in the presence of a large number of other restraints such as NOEs and dihedral angles which, together with secondary structure elements and chemical bonds within each amino acid, help select a single N−H orientation among the possible ones. In the present case, only a good fitting of the back-calculated rdc versus the experimental ones would be enough to assess that the crystal structure is a good model for the solution structure. But this is not the case (see later). An unknown structural change cannot be detected by a single set of rdc. If the measurements are repeated with another lanthanide with a different orienting tensor, another double N−H cone is obtained, with a common apex. The double cones have in common 4 or 8 lines, pairwise differing by 180°. A third lanthanide restricts the orientation of the N−H vector to two opposite directions (this latter ambiguity is intrinsic with the nature of rdc and in practice is irrelevant

(44) Meador, W. E.; Means, A. R.; Quiocho, F. A. *Science* **1993**, *262*, 1718–1721.
(45) Hoeflich, K. P.; Ikura, M. *Cell* **2002**, *108*, 739–742.
(46) Maximciuc, A. A.; Putkey, J. A.; Shamoo, Y.; MacKenzie, K. R. *Structure* **2006**, *14*, 1547–1556.
(47) Schumacher, M. A.; Rivard, A. F.; Bächinger, H. P.; Adelman, J. P. *Nature* **2001**, *410*, 1120–1124.
(48) Aoyagi, M.; Arvai, A. S.; Tainer, J. A.; Getzoff, E. D. *EMBO J.* **2003**, *22*, 766–775.
(49) Liu, M.; Chen, T. Y.; Ahamed, B.; Li, J.; Yau, K. W. *Science* **1994**, *266*, 1348–1354.

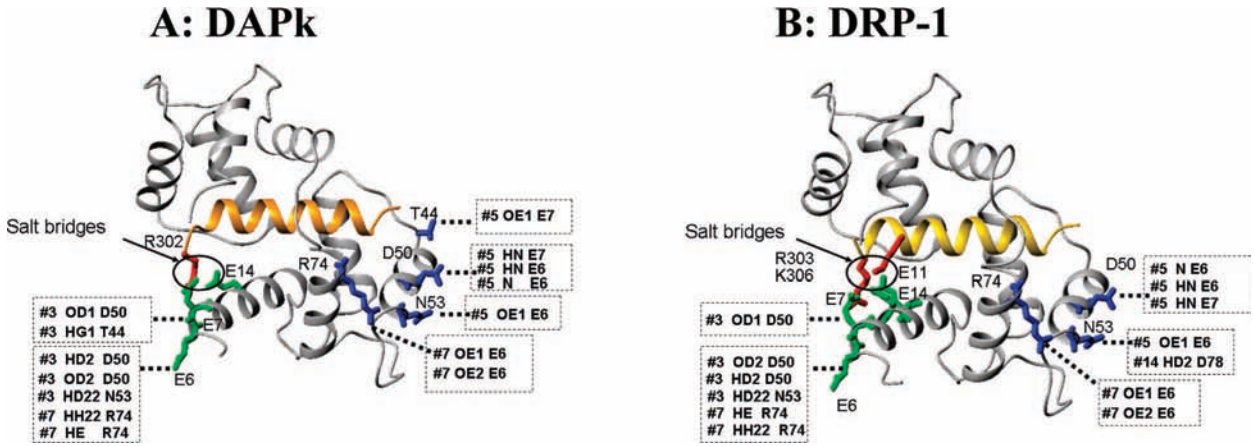

Figure 2. Pattern of H-bonds and salt bridges which are lost or altered on passing from the solid state crystalline form to solution. All the intermolecular H-bonds between the N-terminal domain and neighbor molecules are lost in both complexes.

when the starting structure is sufficiently accurate to have each initial N−H vector much closer to one of the two orientations).

In our strategy, the determination of magnetic susceptibility anisotropies and principal directions relied on eq 2 from the measured pcs and the (initial or final) protein structures. The determination of $\Delta\chi$'s and directions from the independent sets of pcs data allows a straightforward use of eq 1, relating rdc and structural data. Note that there is only one set of orienting tensors for both domains of CaM, i.e., that due to the lanthanides. The orienting tensors could be obtained also from the structure and the rdc through eq 1. However, the tensors obtained from rdc are heavily affected by the initial inaccurate orientations of N−H vectors that are commonly observed in X-ray structures[2] (see Figure S3) and in NMR structures obtained in the absence of rdc,[50] so that the calculated magnetic susceptibility anisotropies are smaller than the actual ones and also the orientations may be somewhat different. This is the reason why we prefer to determine the tensor from pcs, which are only sensitive to the coordinates of the observed nuclei (N and ^{N}H) and not to the orientations of the N−H vectors.[30] As mentioned in the Materials and Methods section, the rdc of the N−H vectors found to experience conformational equilibria between the milli- and microseconds time scale are discarded. Therefore, the use of the actual orienting tensor relates biunivocally rdc and N−H vectors. It should be recalled that, when external orienting media are used, the orienting tensor has to be determined through rdc themselves.

NMR experiments were performed on the N60D variant of CaM, because in this variant the second binding site of its N-terminal domain can selectively bind a paramagnetic lanthanide ion.[6] It has already been shown that Ln substitution and the N60D mutation do not affect the protein structure besides the metal coordination sphere.[6,7,51] As much as long-range electrostatic interactions are concerned, the substitution of the tripositive Ln^{3+} ion for the Ca^{2+} ion is compensated by the additional negative charge introduced next to the metal by the N60D mutation. Pcs of ^{N}H, N nuclei and rdc of the ^{N}H−N pairs for three paramagnetic $LnCa_3CaM$ forms when bound to the DAPk (Ln = Tb, Tm, Yb) or to the DRP-1 (Ln = Tb, Tm, Dy) peptide were measured. All the following analysis is essentially based on three ^{N}H pcs and three ^{N}H−N pair rdc data sets for each of the two complexes. Additional rdc data for a fourth Ln derivative of the DAPk complex (Dy), pcs data for N, Cα, Cβ, C′ for both complexes, and two sets (Ln = Tm, Yb) of C^{α}−H^{α} pair rdc for the DAPk complex were also collected and used as detailed below. The peptides were ignored in the present analysis, except in the solution structure calculations, where they were included as found in the crystal structure and minimized (see Materials and Methods).

Initial Determination of the Magnetic Anisotropy Tensors from Pcs and Inconsistency of the Rdc Data. According to the present strategy, the magnitude and orientation of the Ln-centered magnetic susceptibility tensors is initially calculated by fitting the ^{N}H pcs values of the N-terminal domain (the domain bearing the paramagnetic metal) to the crystal structure through eq 2 (Figure 3A,B and Table 1). Then a first check for consistency of the rdc data with the crystal structure is made through eq 1. If the rdc data were back-calculated satisfactorily, it would be immediately concluded that the solution structure does not differ appreciably from the crystal structure. The calculated rdc, even neglecting those of mobile residues (see the Materials and Methods section), were found to disagree with the experimental values for a relatively large number of residues by much more than the experimental error (Figure 3C,D). As a consequence, these residues should experience a somewhat different conformation in solution with respect to the solid state. The corresponding Q_{free} values are 0.73, 0.52, and 0.53 for Tb, Tm, and Yb rdc, respectively, for the complex with the DAPk peptide, and 0.47, 0.31, and 0.53 for Tb, Tm, and Dy rdc, respectively, for the complex with the DRP1 peptide. It is reiterated that pcs are sufficiently robust to provide the magnetic susceptibility anisotropy tensors, because they are not sensitive to small local conformational changes, and the error in the measurement of amide proton pcs is indeed quite small (0.1 ppm). In contrast to pcs, rdc, even excluding mobility, are very sensitive to small local conformational changes, because they depend on the orientation of the N−^{N}H vectors with respect to the axes of the magnetic susceptibility anisotropy tensor.[50]

The rdc measured for the C-terminal domain for each of the three metal derivatives and each of the two peptide complexes span ranges of values similar to those measured for the N-terminal domain (Figure S4), differently from the free CaM case, when the rdc measured in the C-terminal domain were much smaller than those of the N-terminal domain.[6,7] This

(50) Fischer, M. W.; Losonczi, J. A.; Weaver, J. L.; Prestegard, J. H. *Biochemistry* **1999**, *38*, 9013–9022.
(51) Bertini, I.; Gelis, I.; Katsaros, N.; Luchinat, C.; Provenzani, A. *Biochemistry* **2003**, *42*, 8011–8021.

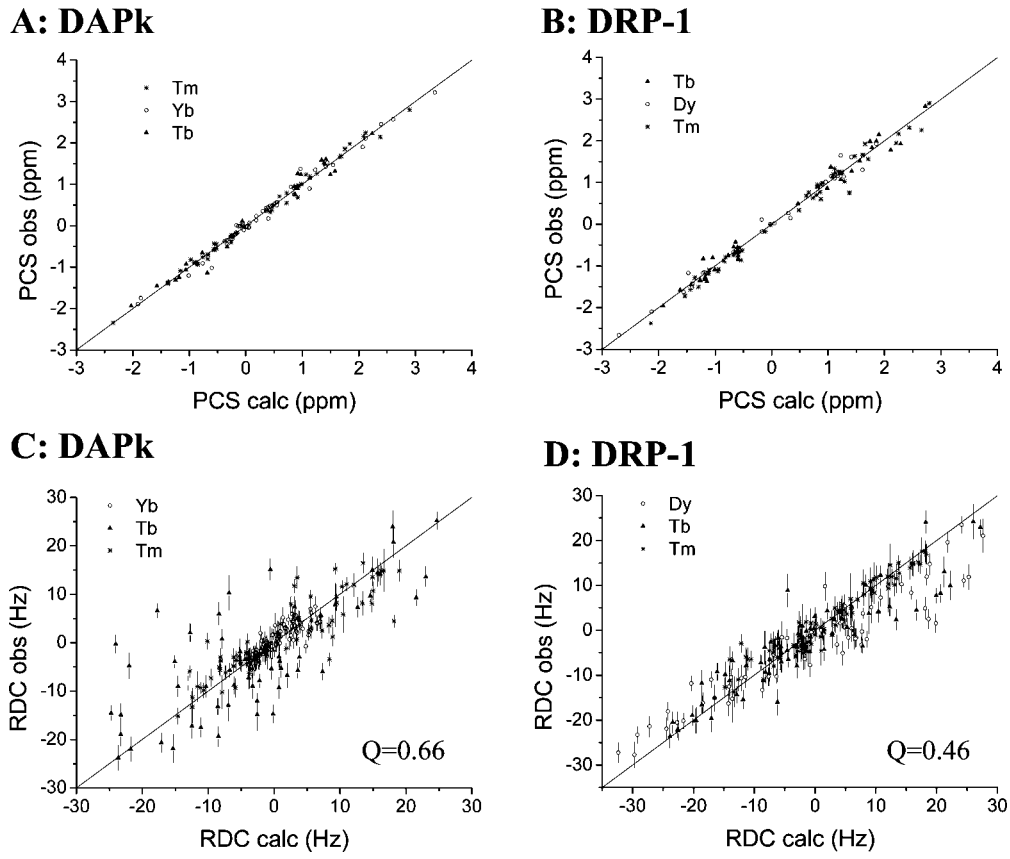

Figure 3. Observed versus calculated pcs of N-terminal domain nuclei for the three lanthanide-substituted CaM samples in the adduct with DAPk (A) and DRP-1 (B) peptides. Calculations have been performed using the protein crystal structure. Observed rdc values versus rdc values calculated using the crystal structure and the paramagnetic susceptibility anisotropy tensor obtained from the fit of the N-terminal domain pcs in the presence of the DAPk (C) or the DRP-1 (D) peptides.

already suggests that in these complexes the two CaM domains are essentially maintaining a fixed conformation with respect to one another upon peptide binding. However, when the two domains are kept rigid as in the crystal structure, no satisfactory fit of the rdc is obtained, while the disagreement for each domain fitted separately is smaller (Figure S5). Therefore, the two domains must have a somewhat different reciprocal orientation in solution with respect to the solid state.

Solution Structure of the N-Terminal Domain. The N-terminal domain contains the orienting lanthanide and can be analyzed independently of the C-terminal domain regardless of whether the latter is rigidly connected to the former or not. Its structure was calculated with the proposed methodology: from the initial magnetic tensors independently obtained from pcs for the three lanthanides, a new structure is obtained through a minimization of both pcs and rdc performed with Xplor-NIH,[52] through PARArestraints for Xplor-NIH[41] (see Materials and Methods). Pcs restraints were given a large weight to essentially fix the directions of the magnetic susceptibility tensors during the whole calculations. Since the diamagnetic chemical shifts are also available, we have also used the dihedral angles obtained through TALOS.[53] They do not induce any significant change in the structure, demonstrating its robustness. The magnetic tensor was recalculated from pcs and the resulting structure with very modest changes (Table 2). The agreement between the structure and both pcs and rdc values was excellent (Figure 4), with Q values for the rdc of 0.11 and 0.21 for the DAPk and DRP-1 peptides, respectively.

Interestingly, besides the expected readjustments of the N−H vector orientations with respect to the X-ray structure,[2,54] the first helix has a significantly different orientation (16°) with respect to the crystal structure. A very similar movement with respect to the X-ray structure was observed by Bax et al. for free CaM in solution using rdc and external orienting media.[2] The same results could be obtained through eq 1 by calculating the magnetic susceptibility anisotropies and main axes directions directly from the rdc and the crystallographic structure and by refining it. However, the final orienting tensors resulted in being significantly smaller (∼10%), and more importantly the directions are off by up to 10° with respect to those obtained from pcs (and even larger for the x and y axes of Yb, due to its low in-plane anisotropy; see Table 1). The consequences on the resulting structure are minor (the rmsd among residues 6−75 between the two structures is ∼0.8 Å), but the orientations of the tensors are less reliable and this would make them unsuitable to detect modest changes in the relative conformation of the two domains with respect to the X-ray structure. For a discussion of the potential unreliability of rdc in two-domain proteins, see also Fischer et al.[50]

Whole Protein Solution Structure. The C-terminal domain was then allowed to both rearrange and reorient with respect to the N-terminal domain while keeping the $\Delta\chi$ tensors fixed and

(52) Schwieters, C. D.; Kuszewski, J.; Tjandra, N.; Clore, G. M. *J. Magn. Reson.* **2003**, *160*, 65–73.
(53) Cornilescu, G.; Delaglio, F.; Bax, A. *J. Biomol. NMR* **1999**, *13*, 289–302.
(54) Chou, J. J.; Li, S.; Bax, A. *J. Biomol. NMR* **2000**, *18*, 217–227.

Table 1. Magnetic Susceptibility Anisotropy Values Calculated by Fitting the Experimental Data to the Crystal Structure and Angles between the *z* and *x* Axes of the Magnetic Susceptibility Anisotropy Tensors[a]

DAPk									
	Tb^{3+}	Tm^{3+}	Yb^{3+}	$z^{Tb}-x^{Tm}$		$x^{Tb}-z^{Tm}$		$z^{Tb}-x^{Yb}$		$x^{Tb}-z^{Yb}$
from N-terminal domain pcs										
$\Delta\chi_{ax}$	35.5	25.1	8.68×10^{-32} m^3	6°		26°		24°		7°
$\Delta\chi_{rh}$	−16.9	−11.0	-1.18×10^{-32} m^3							
				$z-z'\|^{Tb}$	$x-x'\|^{Tb}$	$z-z'\|^{Tm}$	$x-x'\|^{Tm}$	$z-z'\|^{Yb}$	$x-x'\|^{Yb}$	*b*
from N-terminal domain rdc of nonmobile HN										
$\Delta\chi_{ax}$	31.0	24.0	8.90×10^{-32} m^3	13°	26°	8°	7°	2°	1°	*b*
$\Delta\chi_{rh}$	−17.4	−7.8	-0.36×10^{-32} m^3							
from C-terminal domain rdc of nonmobile HN										
$\Delta\chi_{ax}$	30.0	18.7	6.98×10^{-32} m^3	31°	24°	16°	35°	22°	24°	*b*
$\Delta\chi_{rh}$	−12.9	−8.6	-1.90×10^{-32} m^3							
DRP1										
	Tb^{3+}	Tm^{3+}	Dy^{3+}	$z^{Tb}-x^{Tm}$		$x^{Tb}-z^{Tm}$		$z^{Tb}-y^{Dy}$		$x^{Tb}-z^{Dy}$
from N-terminal domain pcs										
$\Delta\chi_{ax}$	37.3	22.7	-40.6×10^{-32} m^3	8°		17°		12°		14°
$\Delta\chi_{rh}$	−14.2	−12.5	19.6×10^{-32} m^3							
				$z-z'\|^{Tb}$	$x-x'\|^{Tb}$	$z-z'\|^{Tm}$	$x-x'\|^{Tm}$	$z-z'\|^{Dy}$	$x-x'\|^{Dy}$	*b*, *c*
				10°	8°	3°	3°			*b*
from N-terminal domain rdc of nonmobile HN										
$\Delta\chi_{ax}$	26.3	22.2	-29.7×10^{-32} m^3	19°	20°	7°	37°	16°	30°	*c*
$\Delta\chi_{rh}$	−19.8	−5.2	12.5×10^{-32} m^3							
from C-terminal domain rdc of nonmobile HN										
$\Delta\chi_{ax}$	30.7	20.6	-32.1×10^{-32} m^3	7°	11°	2°	9°	3°	6°	*c*
$\Delta\chi_{rh}$	−15.0	−8.2	16.5×10^{-32} m^3							

[a] The uncertainties for the magnetic susceptibility anisotropy values are estimated as 10%, and those for the tensor axes directions, as 5°. [b] Angles with respect to the tensor calculated for DAPk from N-terminal domain pcs ($z-z'|^{Tb}$ indicates the angle between the z axis and the corresponding axis of the latter tensor calculated for the Tb derivative, etc.). [c] Angles with respect to the tensor calculated for DRP-1 from N-terminal domain pcs.

Table 2. Magnetic Susceptibility Anisotropy Values Obtained from the N-Terminal Domain Pcs and Refined Solution Structures[a,b]

DAPk							
	Tb^{3+}	Tm^{3+}	Yb^{3+}	z^{Tb}-x^{Tm}	x^{Tb}-z^{Tm}	z^{Tb}-x^{Yb}	x^{Tb}-z^{Yb}
$\Delta\chi_{ax}$	39.4	25.7	8.95×10^{-32} m^3	4°	9°	16°	12°
$\Delta\chi_{rh}$	−15.1	−12.1	-1.27×10^{-32} m^3				
DRP-1							
	Tb^{3+}	Tm^{3+}	Dy^{3+}	z^{Tb}-x^{Tm}	x^{Tb}-z^{Tm}	z^{Tb}-y^{Dy}	x^{Tb}-z^{Dy}
$\Delta\chi_{ax}$	40.0	24.4	-40.3×10^{-32} m^3	5°	11°	9°	19°
$\Delta\chi_{rh}$	−17.1	−13.0	-17.7×10^{-32} m^3				

[a] The uncertainties for the axial component are estimated as 10%, as calculated by removal of different subsets of data. [b] Tensor axes of Tb^{3+} and Tm^{3+} calculated in the presence of the DAPk peptide are all within 3° with respect to those calculated in the presence of the DRP-1 peptide.

equal to those obtained from the pcs-based refinement of the N-terminal domain. A very satisfactory result was obtained with *Q* values for the rdc of the C-terminal domain of 0.11 and 0.13 for the DAPk and DRP-1 cases, respectively. While locally the orientations of the N−H vectors are readjusted with respect to the X-ray structure, as for the N-terminal domain, on a global scale the C-terminal domain is still substantially identical to the crystal structure, except that it is reoriented with respect to the N-terminal domain. The rmsd for the whole structure (residues 6−146) between solid and solution states for the complex with the DAPk peptide is 2.0 Å. This is a remarkable difference, which is largely due to a reciprocal reorientation of the two domains. In fact, the rmsd between solid and solution state structures for the C-terminal domain alone (residues 81−146) is only 0.8 Å, while it is 1.4 Å for the N-terminal domain (residues 6−75), mostly on account of the global movement of the first helix. The corresponding values for the complex with the DRP-1 peptide are 1.1, 0.5, and 0.9 Å. The latter complex is therefore less different from the X-ray structure with respect to the former. The resulting structures are deposited in PDB (2K0J and 2K61) and are shown in Figure 5. Figure 6 shows the agreement between all observed and calculated pcs and rdc data.

In summary, the differences with respect to the crystallographic structures are in the orientation of the first helix of the N-terminal domain and of the whole C-terminal domain, as evidenced by the superimposition of residues 20−65 of the two structures (Figure 5C,D). The first and the second helix of the C-terminal domain (which are almost perpendicular one with respect to the other) are rotated by 13° ± 3° and by 17° ± 3°, respectively, in the complex with the DAPk peptide, and by 5° ± 1.5° and by 5° ± 1.5°, respectively, in the complex with the DRP-1 peptide (for the error determination method, see the Obtaining the Structure in Solution section). For the DRP-1 peptide complex, the rotation of the C-terminal domain is sizably smaller than that for the DAPk peptide complex but in the same direction. Therefore, this type of movement seems characteristic of this class of CaM−peptide complexes, although in the case of the DRP-1 complex the structural change with respect to the crystal structure is closer to the indetermination limit. The movement of the first helix for the DRP-1 peptide complex is significant and similar to that of the DAPk peptide complex.

In the calculations, the peptides were included together with the CaM crystal model, but no restraints have been used (so that they are kept in place by the van der Waals contacts only)

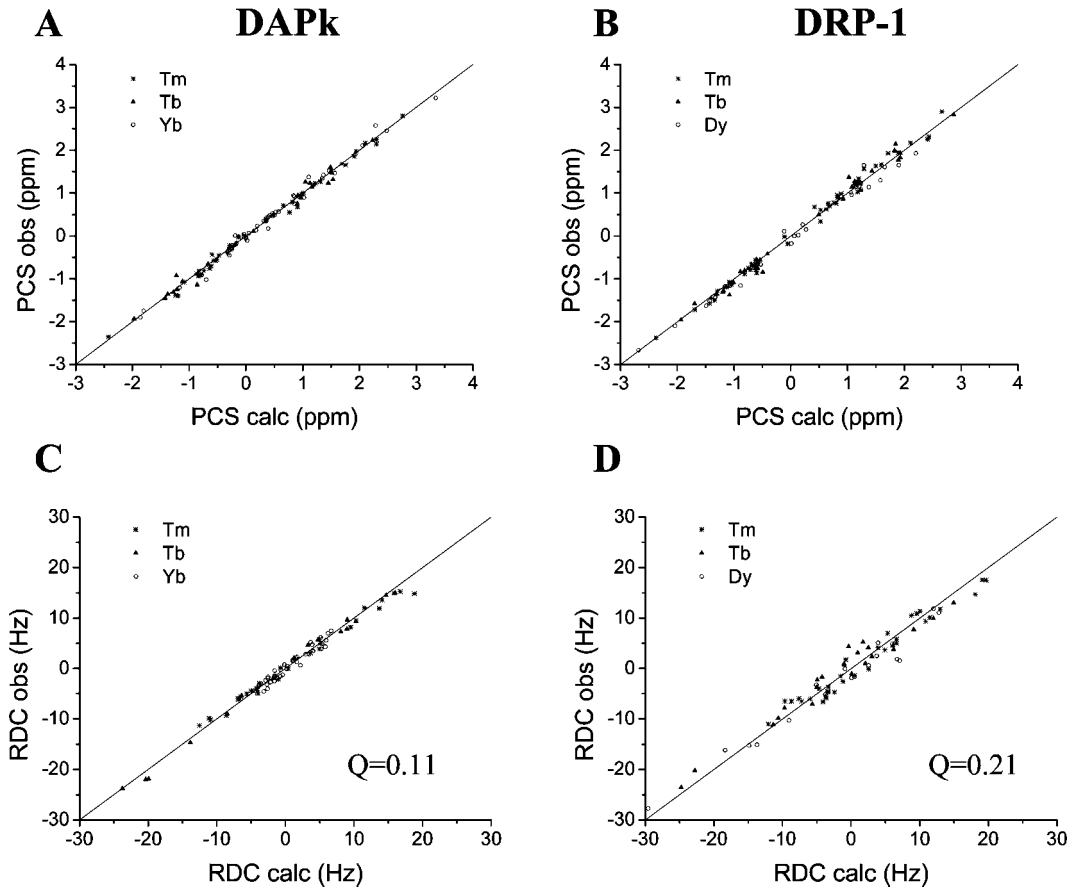

Figure 4. Observed versus calculated N-terminal domain pcs and rdc for the three lanthanide-substituted CaM samples in the adduct with the DAPk peptide (A, C) or the DRP-1 (B, D) peptide, using the solution structure calculated after refinement of the N-terminal domain structure. Corresponding magnetic susceptibility anisotropy tensor parameters are reported in Table 2.

and likewise no restraints are provided involving side-chain nuclei. The same calculations were also repeated without including the peptides, and virtually identical CaM structures were obtained.

If the calculations are made by letting the magnetic susceptibility tensors vary as determined from eq 1 (i.e., ignoring pcs), the covariance between the orienting tensors and the structure is such that the structure is refined by keeping the orientation of the two domains much closer to the solid state orientation (see Supporting Information, Figure S6A). This is due to the fact that the structure readjusts locally to tensors which are different from the "true" ones. Comparison of Figure 6A with Figure S6B shows that such refinement dramatically worsens the agreement with pcs. This exercise shows that rdc alone cannot simultaneously provide reliable local and global refinements, as already observed.[50] The difference from the "true" tensors is much larger than the error which was estimated by performing multiple calculations after removal of one-third of the input pcs and rdc data, perturbed with a stochastic error of 0.1 ppm and 1.5 Hz, respectively. This is proof that when more that one rearrangement is possible, the covariance between orienting tensor parameters and structure should be removed to avoid false minima. On the contrary, structure calculations performed using rdc data and rigid domains fixed to the crystal structure have been shown to be successful in two domain proteins.[4,50] Such calculations are discussed in the Supporting Information (Figure S7A) for the present system. In this case, the relative reorientation of the two domains is even larger than that observed using our strategy, but recalculated pcs values, especially for the N-terminal domain, are in poor agreement with the experimental ones (Figure S7B). The reason for the failure of the rigid domain refinement in the present case is the fact that the N-terminal domain cannot be assumed to maintain the global crystal structure because of the sizable reorientation of the first helix within the domain.[55]

Further Support to the Solution Structures. The solution structure of CaM when bound to the DAPk peptide was also calculated by adding the $C^{\alpha}-H^{\alpha}$ rdc measured for the Yb and Tm CaM derivatives. The obtained structure is in very good agreement with that calculated without such restraints (the orientations of the first and second helix of the C-terminal domain change by less than 3°, i.e., within the standard deviation), and the corresponding rdc values are in excellent agreement with the experimental ones (see Supporting Information, Figure S8).

The quality of the structures can also be monitored using the Q factor[56] calculated from the rdc, which decreases from 0.47 and 0.32, as calculated using the crystal structures of the adduct with DAPk and DRP-1 and the orienting tensors in best

(55) Finally, if calculations are performed using pcs and rdc and defining all helices as rigid domains fixed to the crystal structures, solution structures are calculated very close to the structures previously obtained for the two peptides and shown in Figure 5. This indicates that even without keeping the helices rigid, experimental data are satisfied by a global reorientation of the domains, rather then by uniquely altering the local structure near individual N−H bonds.

(56) Cornilescu, G.; Marquardt, J.; Ottiger, M.; Bax, A. *J. Am. Chem. Soc.* **1998**, *120*, 6836–6837.

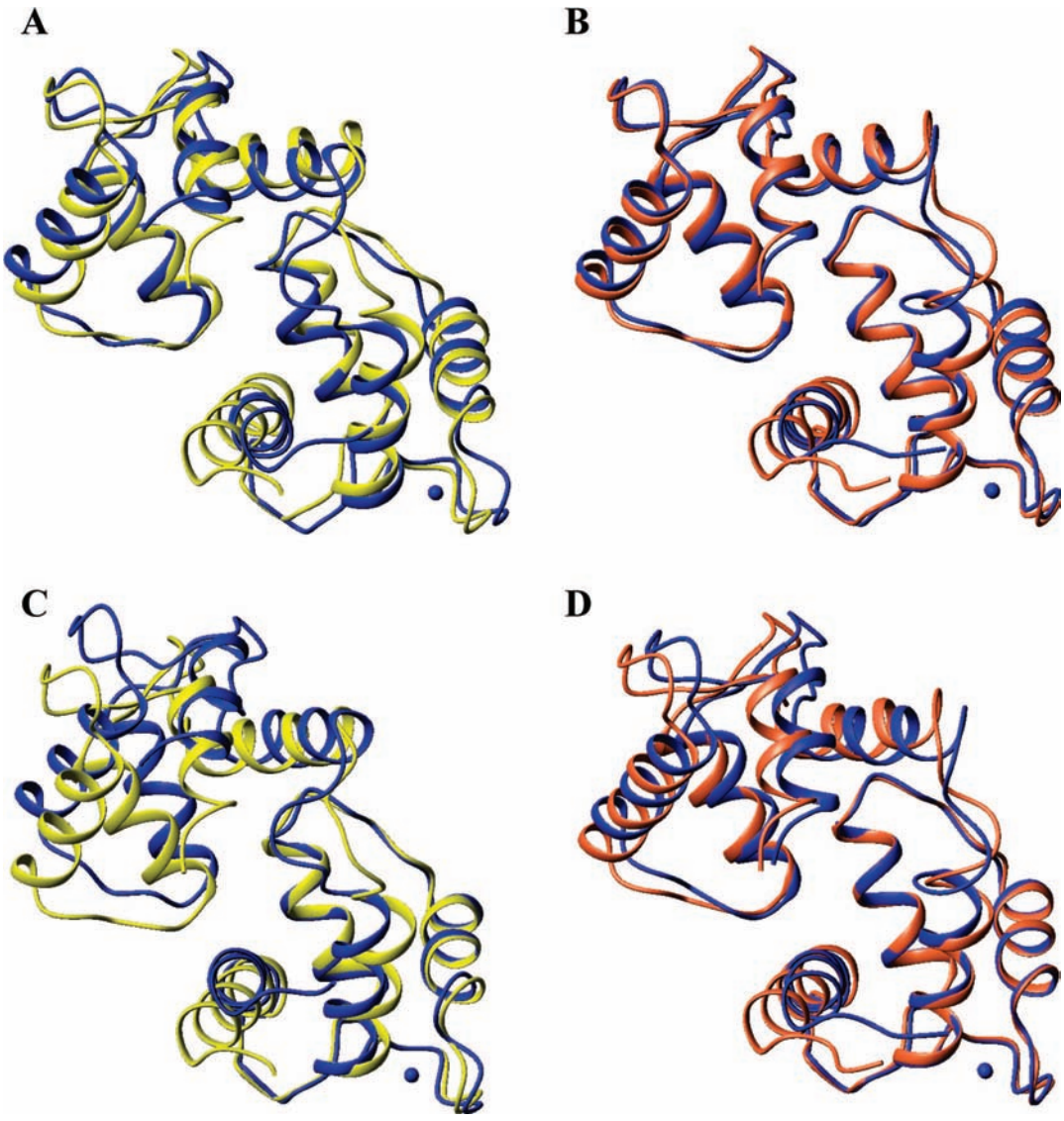

Figure 5. CaM solution structures (in blue) are shown together with the crystal structures (in yellow/orange) calculated in the presence of the DAPk (A, C) or the DRP-1 peptides (B, D). The structures are shown after superimposition of residues in the 6−146 range (A, B) or in the 25−65 range (C, D).

agreement with the crystal structures, to 0.14 and 0.18, as calculated from the refined solution structures of the adduct with DAPk and DRP-1 and the anisotropy susceptibility tensors calculated for the solution structures. A validation of the structure calculated in the presence of the DAPk peptide has been performed by comparing the rdc measured for $DyCa_3CaM$, which were not used in the structure calculations.[2] The Q_{free} factor[56] calculated from the Dy rdc of nonmobile residues decreases from 0.65, as calculated using the crystal structure, to 0.25, as calculated from the refined solution structure, thus indicating an increase in the accuracy of the backbone structure with respect to the crystal structure.[57] A validation of the calculated structure was also performed by comparing the structures obtained using only two of the three sets of pcs and rdc data.[2] Such structures have a backbone rmsd values with a mean of 0.6 and 0.4 Å for the complex in the presence of the DAPk and DRP-1 peptides, respectively (residue range 6−146; see Supporting Information, Figure S9). When calculating the structures by leaving out either one of the two less numerous of the three sets of pcs and rdc data, the Q_{free} factors for the excluded set of rdc data decrease in all cases (Figure S9), thus indicating an increased backbone accuracy with respect to the crystal structure.[57] Finally, the quality of the solution structures is similar to that of the crystal structures, as can be estimated by using PROCHECK_NMR (see Table S3 in the Supporting Information).[58]

It is known that rdc are averaged on time scales larger than that of relaxation times, and therefore more rdc than warranted may be retained because residues have been considered nonmobile if showing no mobility effects only through relaxation measurements. On the other hand, the global changes in the relative orientation of the two domains are determined by the whole ensemble of the rdc, and we have checked that even if one-third of them are randomly removed, similar structures are calculated (data not shown). On the other side, even if all measured rdc, comprising those of N−H vectors identified as mobile through relaxation measurements, are used in the calculations, the calculated structures remain basically the same.

(57) Clore, G. M.; Kuszewski, J. *J. Am. Chem. Soc.* **2003**, *125*, 1518–1525.

(58) Laskowski, R. A.; Rullmann, J. A. C.; MacArthur, M. W.; Kaptein, R.; Thornton, J. M. *J. Biomol. NMR* **1996**, *8*, 477–486.

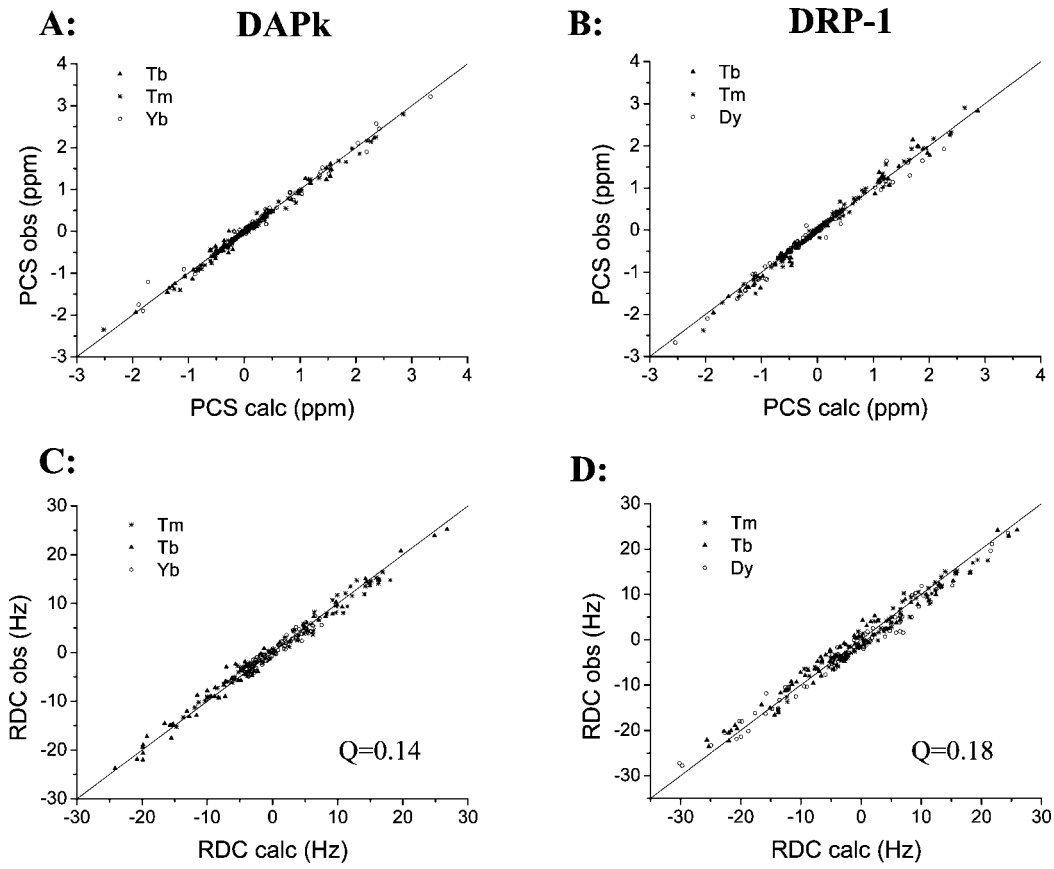

Figure 6. Observed pcs and rdc values versus the values calculated using the solution structures of CaM in the presence of the DAPk (A, C) or the DRP-1 (B, D) peptide.

Therefore, removal of a few more rdc is not expected to alter the picture significantly.

Concluding Remarks

Protein solution structures can be basically coincident, somewhat different, or completely different from their crystal structures. Examples for the third case are, for instance, CaM, MMP, and xylanase Cex;[28,59,60] examples for the second case have already been cited.[2,4,50] In this work, we have shown that the simultaneous use of paramagnetic restraints such as the pcs-derived orientation tensor and self-orientation rdc can discriminate among these cases. For the present systems, pcs and rdc indicated that the solution structures are somewhat different from the crystal structures, and despite the simultaneous rearrangement of different protein parts, we succeeded in determining solution structures of similar quality as the crystal structures and in providing a more accurate description of the corresponding protein structures in solution. This has been possible because the magnetic susceptibility tensors obtained from pcs through eq 2 were used, which are more reliable than those calculated from rdc.

Residual dipolar couplings originating from external orienting media were previously used to detect structural rearrangements in solution with respect to the crystal structure.[2,4,5,54] Their use in two-domain proteins has been also critically discussed.[50] For a two-domain protein such as CaM, paramagnetic rdc offer the advantage that (i) relative conformational freedom can be immediately assessed and, if present, dealt with using the recently developed maximum allowed probability approach;[6,7] (ii) in the absence of significant conformational freedom, the global orientation tensor can be independently and precisely determined from the simultaneous use of pcs; and (iii) the *relative* rearrangement of a domain or a secondary structure element with respect to the metal-binding site can be detected.

Comparative examination of the crystal and solution structures suggests that the main origin for their difference may lie in the loss of the intermolecular hydrogen bonds which, in the crystalline state, tend to keep helix 1 apart from the rest of the N-terminal domain (see Figure 2). As already shown, intermolecular H-bonds are actually present in the crystal state only between the first helix of the N-terminal domain and the third or fourth helix of the N-terminal domain of a neighboring molecule (E6-D50, E6-N53, E6-R74, E7-T44, E7-D50). When these intermolecular interactions are lost in solution, helix 1 moves closer to the rest of the N-terminal domain (as already observed in free CaM[2]). The occurrence of salt bridges observed in the crystal structure between the N-terminal portion of the bound peptide and both the first helix of the N-terminal domain of CaM and glutamates in the C-terminal domain of CaM may then facilitate the change in orientation of the C-terminal domain of CaM, observed in the solid state with respect to the solution structure. Interestingly, while the movement of the first N-terminal helix from solid state to solution is very similar for the two complexes, in agreement with the same kind of crystal packing forces in the two crystal lattices (the two complexes

(59) Poon, D. K. Y.; Withers, S. G.; McIntosh, L. P. *J. Biol. Chem.* **2007**, *282*, 2091–2100.
(60) Bertini, I.; Calderone, V.; Fragai, M.; Jaiswal, R.; Luchinat, C.; Melikian, M.; Mylonas, E.; Svergun, D. *J. Am. Chem. Soc.* **2008**, *130*, 7011–7021.

crystallize in the same space group), the movement of the C-terminal domain is more marked for the DAPk than for the DRP-1 complex, as if the crystal packing distortion is transmitted less well from the N-terminal to the C-terminal domain through the different bound peptide.

Substitution of a lanthanide in a metal binding site may be in principle successful everytime there is a metal binding site. Furthermore, lanthanides may be also helpful when using rigid[14−17] paramagnetic tags.[8,61−63] This approach is particularly useful for proteins with domains experiencing flexibility, such as multidomain proteins, and for protein−protein adducts. However, the same approach can also be applied to detect significant structural differences in single domain proteins containing a metal ion binding site, either natural or artificial, and is, therefore, quite general.

Finally, it should be mentioned that ensemble average approaches have been recently introduced to improve the agreement in the fit of the rdc data when needed.[64−69] In our case, the data are fitted reasonably well with the assumption of a unique structure. However, this does not rule out that a more complex treatment would provide more information on the actual system in solution. In such cases, the determination of the orientation tensor from pcs would provide an even more distinct advantage, given that rdc will be heavily averaged by the different orientations of the N−H vectors in the different members of the ensemble, while the coordinates of the N and ^{N}H nuclei in the tensor frame, and therefore the pcs values, will be much less affected.

Acknowledgment. Stimulating discussions and helpful suggestions by Christian Griesinger are acknowledged. We thank Mr. Paul Ionescu for providing apo-calmodulin samples and Inaki de Diego for discussions. This work has been supported by Ente Cassa di Risparmio, MIUR-FIRB Contracts RBLA032ZM7 and RBIP06LSS2, and by European Commission, Contracts EU-NMR 026145, SPINE2-COMPLEXES 031220, and LSHG-CT-2004-512052.

Supporting Information Available: Diffraction data collection and crystal structure refinement statistics for CaM bound to the DRP-1 peptide. Statistics provided by PROCHECK-NMR. ^{N}H pcs and ^{N}H−N rdc of CaM residues in the adducts. TALOS angle restraints. CaM residues with mobile NH vectors identified by relaxation rate measurements. H-bonds, salt bridges, and van der Waals contacts between the CaM peptide complexes and their neighbors in the crystalline state. R_1 and R_2 measurements. A simulation addressing the different accuracy of pcs- and rdc-derived tensors in the presence of N−H orientation inaccuracies. Observed rdc values versus rdc values calculated using the crystal structures. Solution structures obtained by including in the calculation the rdc restraints alone, and the C^{α}−H^{α} rdc. Structures calculated using subsets of restraints. Xplor script for the refinement of the crystal structure using pcs and rdc restraints. This material is available free of charge via the Internet at http://pubs.acs.org.

JA8080764

(61) Wöhnert, J.; Franz, K. J.; Nitz, M.; Imperiali, B.; Schwalbe, H. *J. Am. Chem. Soc.* **2003**, *125*, 13338–13339.
(62) Prudencio, M.; Rohovec, J.; Peters, J. A.; Tocheva, E.; Boulanger, M. J.; Murphy, M. E.; Hupkes, H. J.; Koster, W.; Impagliazzo, A.; Ubbink, M. *Chem.−Eur. J.* **2004**, *5*, 3252–3260.
(63) Ikegami, T.; Verdier, L.; Sakhaii, P.; Grimme, S.; Pescatore, P.; Saxena, K.; Fiebig, K. M.; Griesinger, C. *J. Biomol. NMR* **2004**, *29*, 339–349.
(64) Iwahara, J.; Schwieters, C. D.; Clore, G. M. *J. Am. Chem. Soc.* **2004**, *126*, 5879–5896.
(65) Clore, G. M.; Schwieters, C. D. *J. Am. Chem. Soc.* **2004**, *126*, 2923–2938.
(66) Clore, G. M.; Schwieters, C. D. *J. Mol. Biol.* **2006**, *355*, 879–886.
(67) Gsponer, J.; Hopearuoho, H.; Whittaker, S. B.-M.; Spence, G. R.; Moore, G. R.; Paci, E.; Radford, S. E.; Vendruscolo, M. *Proc. Natl. Acad. Sci. U.S.A* **2006**, *103*, 99–104.
(68) Lange, O. F.; Lakomek, N.-A.; Farès, C.; Schröder, G. F.; Walter, K. F. A.; Becker, S.; Meiler, J.; Grubmüller, H.; Griesinger, C.; de Groot, B. L. *Science* **2008**, *320*, 1471–1475.
(69) Lindorff-Larsen, K.; Best, R. B.; DePristo, M. A.; Dobson, C. M.; Vendruscolo, M. *Nature* **2005**, *433*, 128–132.